

Beyond Diagonal RIS: Key to Next-Generation Integrated Sensing and Communications?

Tara Esmaeilbeig, Kumar Vijay Mishra and Mojtaba Soltanalian

Abstract—Reconfigurable intelligent surface (RIS) have introduced unprecedented flexibility and adaptability toward smart wireless channels. Recent research on integrated sensing and communication (ISAC) systems has demonstrated that RIS platforms enable enhanced signal quality, coverage, and link capacity. In this paper, we explore the application of fully-connected beyond diagonal RIS (BD-RIS) to ISAC systems. BD-RIS introduces additional degrees of freedom by allowing non-zero off-diagonal elements for the scattering matrix, potentially enabling further functionalities and performance enhancements. In particular, we consider the joint design objective of maximizing the weighted sum of the signal-to-noise ratio (SNR) at the radar receiver and communication users by leveraging the extra degrees-of-freedom offered in the BD-RIS setting. These degrees-of-freedom are unleashed by formulating an alternating optimization process over known and auxiliary (latent) variables of such systems. Our numerical results reveal the advantages of deploying BD-RIS in the context of ISAC and the effectiveness of the proposed algorithm by improving the SNR values for both radar and communication users by several orders of magnitude.

Index Terms—Fully-connected RIS, ISAC, non-convex optimization, NLoS sensing, smart radio environment.

I. INTRODUCTION

Reconfigurable intelligent surfaces (RIS) have demonstrated great potential in realizing smart programmable environments by modifying wireless channels [1, 2] and establishing reliable links for communication and sensing [3]. In particular, RIS have been designed to enhance energy efficiency [4], physical security [5, 6], radar target estimation and detection [7], and facilitate integrated sensing and communications (ISAC) [8, 9]. In this paper, we focus on RIS-enabled ISAC.

ISAC improves spectrum access and usage while reducing both hardware, power, and signaling costs [10–12]. The literature indicates that RIS benefits ISAC in both line-of-sight (LoS) and non-LoS (NLoS) scenarios [13]. When LoS links exist between base station (BS) to communications users or radar targets, RIS is used to compensate for the propagation loss [14, 15]. When the LoS to either users or targets is blocked, RIS is utilized to establish a virtual LoS or NLoS link to bypass the obstructions [16, 17].

Tara Esmaeilbeig and Mojtaba Soltanalian are with the ECE Department, University of Illinois at Chicago, Chicago, IL 60607 USA. Email: {zesmae2, msol}@uic.edu. Kumar Vijay Mishra is with the United States DEVCOM Army Research Laboratory, Adelphi, MD 20783 USA. E-mail: kvm@ieee.org.

This work was sponsored by the Army Research Office, accomplished under Grant Number W911NF-22-1-0263. The views and conclusions contained in this document are those of the authors and should not be interpreted as representing the official policies, either expressed or implied, of the Army Research Office or the U.S. Government. The U.S. Government is authorized to reproduce and distribute reprints for Government purposes notwithstanding any copyright notation herein.

All of the above-mentioned works employ conventional RIS architecture characterized by a diagonal scattering matrix (D-RIS), also known as phase shift matrix. In D-RIS each element is controlled by a tunable impedance connected to ground. Whereas in [18], beyond diagonal RIS (BD-RIS) is introduced by connecting the elements of RIS to each other through a reconfigurable impedance network. When all or a group of the elements are connected to each other the BD-RIS is called fully-connected or group-connected BD-RIS, respectively. The maximum degrees-of-freedom offered by the fully-connected BD-RIS has shown great potential in meeting the upper bound of received signal power in [19]. BD-RIS extends the concept of conventional RIS by actively manipulating the cross-polarization components, inter-element coupling, and coherent scattering effects [20, 21]. By dynamically adjusting these off-diagonal elements, beyond-diagonal RIS reshapes the wavefront in ways previously unattainable, empowering ISAC systems with enhanced resolution, interference suppression, and target discrimination capabilities [22–24]. In this paper, we explore the benefit of fully-connected BD-RIS in ISAC applications. In general, ISAC systems may follow communications-centric design, radar-centric or integrated design [25]. Prior works, including [23], have focused on radar-centric design of BD-RIS for ISAC by maximizing the target detection probability subject to a minimum quality of service at communications users.

Contrary to these studies, we employ a joint communications and sensing design that offers a tunable trade-off between communications and sensing performance. In particular, our design criterion is a weighted sum of the signal-to-noise ratio (SNR) at the communications and radar (sensing) receivers. This approach of weighted joint criterion has previously been considered in ISAC system design studies [26, 27]. We show that optimization of this objective with respect to the hardware constraints of fully-connected BD-RIS is nonconvex. In order to tackle the resulting complicated non-convex optimization problem, we develop an efficient alternating optimization algorithm following a penalty-based framework for unimodular quartic optimization over a finite alphabet set. Our numerical simulations, study the performance of BD-RIS with different number of resolution bits. Additionally, we illustrate that the BD-RIS outperforms the D-RIS with the same number of reflecting elements in terms of enhancing the communications SNR, radar SNR, and, hence, their weighted sum.

Throughout this paper, we use bold lowercase and bold uppercase letters for vectors and matrices, respectively. The identity matrix of size $s \times s$ is denoted by \mathbf{I}_s . The sets of complex and real numbers are \mathbb{C} and \mathbb{R} , respectively; $(\cdot)^T$

and $(\cdot)^H$ are the vector/matrix transpose and the Hermitian transpose, respectively; trace of a matrix is $\text{Tr}(\cdot)$. The Kronecker product is denoted by \otimes . The vectorized form of a matrix \mathbf{B} is written as $\text{vec}(\mathbf{B})$. The maximum eigenvalue of \mathbf{B} is denoted by $\lambda_{\max}(\mathbf{B})$. The angle/phase and real part of a complex number is denoted by $\arg(\cdot)$ and $\text{Re}(\cdot)$, respectively. The operation $\text{vec}_{K,L}^{-1}(\mathbf{c})$ reshapes the input vector $\mathbf{c} \in \mathbb{C}^{KL}$ into a matrix $\mathbf{C} \in \mathbb{C}^{K \times L}$ such that $\text{vec}(\mathbf{C}) = \mathbf{c}$. For a symmetric $n \times n$ matrix \mathbf{A} , the half-vectorization, denoted by $\text{vech}(\mathbf{A})$, is the $(n(n+1)/2) \times 1$ column vector obtained by vectorizing only the lower triangular part of \mathbf{A} i.e. $\text{vech}(\mathbf{A}) = [\mathbf{A}_{1,1}, \dots, \mathbf{A}_{n,1}, \mathbf{A}_{2,2}, \dots, \mathbf{A}_{n,2}, \dots, \mathbf{A}_{n-1,n-1}, \mathbf{A}_{n,n-1}, \mathbf{A}_{n,n}]^T$. Moreover, the unique *duplication* matrix \mathbf{D}_n transforms $\text{vech}(\mathbf{A})$ into $\text{vec}(\mathbf{A})$ as $\text{vec}(\mathbf{A}) = \mathbf{D}_n \text{vech}(\mathbf{A})$.

II. SYSTEM MODEL

Consider a BD-RIS-enabled ISAC system (Fig. 1) comprising a dual-function base station (DFBS) with N elements each in transmit (Tx) and receive (Rx) antenna arrays. The BD-RIS comprises $L = L_x \times L_y$ reflecting elements arranged as a uniform planar array (UPA) with L_x (L_y) elements along the x- (y-) axes in the Cartesian coordinate plane. Define the RIS steering vector $\mathbf{a}(\theta_h, \theta_v) = \mathbf{a}_x(\theta_h, \theta_v) \otimes \mathbf{a}_y(\theta_h, \theta_v)$, where θ_h (θ_v) is the azimuth (elevation) angle, $\mathbf{a}_x(\theta_h, \theta_v) = [1, e^{j\frac{2\pi d}{\lambda} \cos\theta_h \sin\theta_v}, \dots, e^{j\frac{2\pi d(L_x-1)}{\lambda} \cos\theta_h \sin\theta_v}]^T$ and $\mathbf{a}_y(\theta_h, \theta_v) = [1, e^{j\frac{2\pi d}{\lambda} \cos\theta_h \sin\theta_v}, \dots, e^{j\frac{2\pi d(L_y-1)}{\lambda} \cos\theta_h \sin\theta_v}]^T$, $\lambda = c/f_c$ is the carrier wavelength, $c = 3 \times 10^8$ m/s is the speed of light, f_c is the carrier frequency, and $d = 0.5\lambda$ is the inter-element spacing. The fully-connected BD-RIS operation is characterized by the scattering or phase matrix Φ which is a complex symmetric unitary, i.e.,

$$\Phi = \Phi^T \text{ and } \Phi^H \Phi = \mathbf{I}. \quad (1)$$

The phases may be assumed continuous or discrete/quantized. In general, discrete phase settings simplify the hardware implementation and control/programming of the RIS. Since discrete phase states are achieved using digital switches or phase shifters, power consumption is lower than continuously variable analog counterparts. For discrete-valued phases with resolution M , we have $[\Phi]_{kl} \in \Omega_M$, where

$$\Omega_M = \left\{ s = e^{j\omega}, \omega \in \Pi_M \right\}, \quad (2)$$

$$\Pi_M = \left\{ 1, \frac{2\pi}{M}, \dots, \frac{2\pi(M-1)}{M} \right\}.$$

The continuous BD-RIS is equivalent to the discrete RIS with infinite resolution i.e. $M \rightarrow \infty$ [28]. In other words, we have $[\Phi]_{kl} \in \Omega$ where $\Omega = \{s = e^{j\omega}, \omega \in [0, 2\pi)\}$. In this paper, to achieve a discrete-valued BD-RIS phase design, we obtain the optimal phases on the set Ω and then project the solution onto the set Ω_M .

We now describe the received communications signal at the users and the sensing signal back-scattered from the target and received at the DFBS.

Communications Rx signal: Denote the direct or LoS channel state information (CSI) and RIS-reflected non-line-of-sight

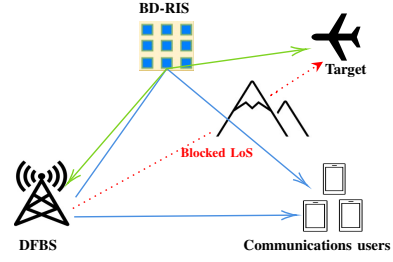


Fig. 1. A illustration of BD-RIS-enabled ISAC system. When the LoS is blocked, the NLoS paths via the BD-RIS allow for establishing the link between the targets/users with the DFBS.

(NLoS) CSI matrices by $\mathbf{F} \in \mathbb{C}^{K \times N}$ and $\mathbf{H} \in \mathbb{C}^{K \times L}$, respectively. Then, at each communications receiver after sampling, the discrete-time received signal is $\mathbf{y}_{c,k}$. Concatenating the received signals from all users, we obtain the $K \times 1$ vector:

$$\mathbf{y}_c = (\mathbf{F} + \mathbf{H}\Phi\mathbf{G})\mathbf{P}\mathbf{s} + \mathbf{n}_c, \quad (3)$$

where $\mathbf{P} \in \mathbb{C}^{N \times K}$ is the DFBS precoder, the Tx-RIS CSI matrix $\mathbf{G} \in \mathbb{C}^{L \times N}$ is assumed to be estimated *a priori* through suitable channel estimation techniques and $\mathbf{n}_c \sim \mathcal{N}(\mathbf{0}, \sigma_c^2 \mathbf{I}_K)$ is the spatially and temporally white noise at communications receivers.

Sensing Rx signal at DFBS: Consider a Swerling-0 [29] radar target located at a NLoS location with respect to the DFBS. The direction-of-arrival (DoA) is $(\theta_{h_t}, \theta_{v_t})$ with respect to the RIS and radar cross-section (RCS) α_T . Define $\mathbf{R} = \alpha_T \mathbf{G}^T \Phi \mathbf{a}(\theta_{h_t}, \theta_{v_t}) \mathbf{a}(\theta_{h_t}, \theta_{v_t})^T \Phi \mathbf{G}$.

Stacking the echoes for all receiver antennas, the $N \times 1$ signal at radar receiver after down conversion and sampling is

$$\mathbf{y}_r = \mathbf{R}\mathbf{P}\mathbf{s} + \mathbf{n}_r, \quad (4)$$

where $\mathbf{n}_r \sim \mathcal{N}(\mathbf{0}, \sigma_r^2 \mathbf{I}_N)$ is the noise at radar receiver.

Denote $\mathbf{C} = \mathbf{F} + \mathbf{H}\Phi\mathbf{G}$. The output SNR at communications and DFBS Rx are, respectively,

$$\text{SNR}_c = \frac{1}{\sigma_c^2} \text{Tr}(\mathbf{C}\mathbf{P}\mathbf{P}^H \mathbf{C}^H), \text{ and} \quad (5)$$

$$\text{SNR}_r = \frac{1}{\sigma_r^2} \text{Tr}(\mathbf{R}\mathbf{P}\mathbf{P}^H \mathbf{R}^H). \quad (6)$$

In the next section, we use (5)-(6) to formalize the design problem for BD-RIS-enabled ISAC system.

III. BD-RIS DESIGN FOR ISAC

As the design criterion under BD-RIS hardware constraints (1) and (2), we use the weighted sum of the radar and communications SNRs, with a weight factor β as $\text{SNR}_T = \beta \text{SNR}_r + (1 - \beta) \text{SNR}_c$. Our design problem is

$$\begin{aligned} \mathcal{P}_1 : & \text{maximize } \text{SNR}_T \\ & \Phi \in \Omega_M^{L \times L} \\ & \text{subject to } \Phi^H \Phi = \mathbf{I} \text{ and } \Phi = \Phi^T. \end{aligned} \quad (7)$$

Since Φ is symmetric, we solve \mathcal{P}_1 w.r.t $\phi = \text{vech}(\Phi) \in \Omega_M^{L(L+1)/2}$ by means of a penalty-based optimization method. Following Lemmata 1 and 2, state that the SNR at communications and the radar receivers are quadratic and quartic with respect to ϕ , respectively.

Lemma 1. For a symmetric scattering matrix Φ ,

$$\text{SNR}_c = \phi^H \tilde{\mathbf{Q}} \phi + 2 \text{Re}(\mathbf{q}^H \phi) + \mathbf{f}^H \hat{\mathbf{P}} \mathbf{f}, \quad (8)$$

where $\tilde{\mathbf{Q}} = \mathbf{D}_L^\top (\mathbf{G}^H \otimes \mathbf{H})^H \hat{\mathbf{P}} (\mathbf{G}^H \otimes \mathbf{H}) \mathbf{D}_L$, with \mathbf{D}_L denoting the duplication matrix for Φ , and $\hat{\mathbf{P}} = \frac{1}{\sigma_c^2} (\mathbf{P}^\top \otimes \mathbf{I}_K)^H (\mathbf{P}^\top \otimes \mathbf{I}_K)$. Also, $\mathbf{q} = \mathbf{D}_L^\top (\mathbf{G}^H \otimes \mathbf{H})^H \hat{\mathbf{P}} \mathbf{f}$.

Proof: From (5) we have

$$\begin{aligned} \text{SNR}_c &= \frac{1}{\sigma_c^2} \text{Tr}(\mathbf{C} \mathbf{P} \mathbf{P}^H \mathbf{C}^H) = \frac{1}{\sigma_c^2} \text{vec}(\mathbf{C} \mathbf{P})^H \text{vec}(\mathbf{C} \mathbf{P}) \\ &= \frac{1}{\sigma_c^2} \text{vec}(\mathbf{C})^H (\mathbf{P}^\top \otimes \mathbf{I}_K)^H (\mathbf{P}^\top \otimes \mathbf{I}_K) \text{vec}(\mathbf{C}) \\ &= \text{vec}(\mathbf{C})^H \hat{\mathbf{P}} \text{vec}(\mathbf{C}) \\ &= \mathbf{f}^H \mathbf{Q} \mathbf{f} + \mathbf{f}^H \hat{\mathbf{P}} (\mathbf{G}^H \otimes \mathbf{H}) \phi + \phi^H (\mathbf{G}^H \otimes \mathbf{H})^H \hat{\mathbf{P}} \mathbf{f} \\ &\quad + \phi^H (\mathbf{G}^H \otimes \mathbf{H})^H \hat{\mathbf{P}} (\mathbf{G}^H \otimes \mathbf{H}) \phi, \end{aligned} \quad (9)$$

where the last equality used $\text{vec}(\mathbf{C}) = \text{vec}(\mathbf{F}) + (\mathbf{G}^H \otimes \mathbf{H}) \text{vec}(\Phi) = \mathbf{f} + (\mathbf{G}^H \otimes \mathbf{H}) \mathbf{D}_L \phi$. Substituting $\tilde{\mathbf{Q}}$ and \mathbf{q} in (9) yields (8). ■

Lemma 2. For a symmetric scattering matrix Φ ,

$$\text{SNR}_r = \phi^H \bar{\mathbf{Q}}(\Phi) \phi, \quad (10)$$

where

$$\begin{aligned} \bar{\mathbf{Q}}(\Phi) &= \mathbf{D}_L^\top \left(\mathbf{G}^\top \otimes \mathbf{G}^\top \Phi \mathbf{a}(\theta_{h_t}, \theta_{v_t}) \mathbf{a}^\top(\theta_{h_t}, \theta_{v_t}) \right)^H \bar{\mathbf{P}} \\ &\quad \left(\mathbf{G}^\top \otimes \mathbf{G}^\top \Phi \mathbf{a}(\theta_{h_t}, \theta_{v_t}) \mathbf{a}^\top(\theta_{h_t}, \theta_{v_t}) \right) \mathbf{D}_L, \end{aligned} \quad (11)$$

$$\bar{\mathbf{P}} = \frac{|\alpha_T|^2}{\sigma_r^2} (\mathbf{P}^\top \otimes \mathbf{I}_N)^H (\mathbf{P}^\top \otimes \mathbf{I}_N). \quad (12)$$

Proof: From (6) we have

$$\begin{aligned} \text{SNR}_r &= \frac{1}{\sigma_r^2} \text{Tr}(\mathbf{R} \mathbf{P} \mathbf{P}^H \mathbf{R}^H) = \frac{1}{\sigma_r^2} \text{vec}(\mathbf{R} \mathbf{P})^H \text{vec}(\mathbf{R} \mathbf{P}) \\ &= \frac{1}{\sigma_r^2} \text{vec}(\mathbf{R})^H (\mathbf{P}^\top \otimes \mathbf{I}_N)^H (\mathbf{P}^\top \otimes \mathbf{I}_N) \text{vec}(\mathbf{R}) \\ &= \phi^H \bar{\mathbf{Q}}(\Phi) \phi, \end{aligned} \quad (13)$$

where the last equality used $\text{vec}(\mathbf{R}) = \alpha_T \text{vec}(\mathbf{G}^\top \Phi \mathbf{a}(\theta_{h_t}, \theta_{v_t}) \mathbf{a}^\top(\theta_{h_t}, \theta_{v_t}) \Phi \mathbf{G}) = \alpha_T (\mathbf{G}^\top \otimes \mathbf{G}^\top \Phi \mathbf{a}(\theta_{h_t}, \theta_{v_t}) \mathbf{a}^\top(\theta_{h_t}, \theta_{v_t})) \mathbf{D}_L \phi$. ■

From Lemma 1-2, we conclude that the objective function in \mathcal{P}_1 is quartic w.r.t Φ . Define $f(\phi) = \text{SNR}_T = \beta \phi^H \tilde{\mathbf{Q}}(\phi) \phi + (1 - \beta) \phi^H \tilde{\mathbf{Q}} \phi + 2(1 - \beta) \text{Re}(\mathbf{q}^H \phi)$. In order to reduce the problem from quartic to quadratic optimization we introduce a latent (auxiliary) variable $\Phi_0 \in \Omega^{L \times L}$ as a symmetric matrix. Define the new objective as

$$\begin{aligned} f(\phi, \phi_0) &= \beta \phi^H \bar{\mathbf{Q}}(\Phi_0) \phi + (1 - \beta) \phi^H \tilde{\mathbf{Q}} \phi \\ &\quad + 2(1 - \beta) \text{Re}(\mathbf{q}^H \phi). \end{aligned} \quad (14)$$

In order to have the surrogate objective equal to the original objective, i.e. $f(\phi, \phi_0) = f(\phi)$, we propose to optimize $f(\phi, \phi_0)$ under the constraint $\phi = \phi_0$, where $\phi_0 = \text{vech}(\Phi_0)$.

Additionally, in order to impose the constraint $\Phi \in \Omega_{L \times L}^{M \times M}$ in (7), we introduce a second latent variable, $\Phi_1 \in \Omega_M^{M \times M}$ as a symmetric matrix and impose $\Phi = \Phi_1$. Denote $\phi_1 = \text{vech}(\Phi_1)$. In order to impose the unitarity constraint on Φ in \mathcal{P}_1 , we introduce a third auxiliary variable \mathbf{U} with the

constraints $\mathbf{U} = \Phi$ and $\mathbf{U}^H \mathbf{U} = \mathbf{I}$. Introducing these auxiliary variables into problem \mathcal{P}_1 , we obtain the equivalent problem

$$\begin{aligned} \mathcal{P}_2 : \quad & \text{maximize}_{\phi, \phi_0, \phi_1, \mathbf{U}} f(\phi, \phi_0) \\ & \text{subject to } \phi = \phi_0 = \phi_1 = \text{vech}(\mathbf{U}), \end{aligned} \quad (15)$$

$$\mathbf{U}^H \mathbf{U} = \mathbf{I}, \quad (16)$$

$$\phi, \phi_0 \in \Omega^{L(L+1)/2} \text{ and } \phi_1 \in \Omega_M^{L(L+1)/2}. \quad (17)$$

We solve this non-convex problem using the framework proposed in [30] for unimodular quadratic optimization.

IV. OPTIMIZATION FRAMEWORK

The Lagrangian of \mathcal{P}_2 is

$$\begin{aligned} \mathcal{L}(\phi, \phi_0, \phi_1, \mathbf{U}) &= -f(\phi, \phi_0) + \sum_{i=0}^1 \frac{\rho_i}{2} \|\phi_i - \phi\|_2^2 \\ &\quad + \frac{\rho_2}{2} \|\text{vec}(\mathbf{U}) - \phi\|_2^2, \end{aligned} \quad (18)$$

where $\rho_i > 0$, $i \in \{0, \dots, 3\}$ are penalty parameters. Next, we employ a penalty based framework and determine $(\phi, \phi_0, \phi_1, \mathbf{U})$ in an alternating iterative fashion to minimize $\mathcal{L}(\phi, \phi_0, \phi_1, \mathbf{U})$ under the constraints in (16)-(17).

Update of ϕ : With fixed $\phi_0^{(r)}, \phi_1^{(r)}, \mathbf{U}^{(r)}$ at iteration r we need to minimize $\mathcal{L}(\phi, \phi_0^{(r)}, \phi_1^{(r)}, \mathbf{U}^{(r)})$ w.r.t ϕ , which from (14)-(18), is equivalent to

$$\text{minimize}_{\phi \in \Omega^{L(L+1)/2}} \phi^H \mathbf{R}^{(r)} \phi + \text{Re}(\mathbf{c}^{(r)H} \phi) \quad (19)$$

where $\mathbf{R}^{(r)} = -\beta \bar{\mathbf{Q}}(\phi_0^{(r)}) + (\beta - 1) \tilde{\mathbf{Q}}$ and $\mathbf{c}^{(r)} = 2(\beta - 1) \mathbf{q} - \sum_{i=0}^1 \rho_i \phi_i^{(r-1)} - \rho_2 \text{vec}(\mathbf{U})$. (19) is equivalent to

$$\text{minimize}_{\bar{\phi} \in \Omega^{L(L+1)/2+1}} \bar{\phi}^H \mathbf{A}^{(r)} \bar{\phi}, \quad (20)$$

where $\mathbf{A}^{(r)} = \begin{bmatrix} \mathbf{R}^{(r)} & \mathbf{c}^{(r)}/2 \\ \mathbf{c}^{(r)H}/2 & 0 \end{bmatrix}$ and $\bar{\phi} = [\phi^\top \ 1]^\top$.

This problem with feasible set $\Omega^{L(L+1)/2+1}$ is a unimodular quadratic program for which the following iterations will lead to non-increasing objective

$$\bar{\phi}^{(r,s+1)} = e^{j \arg(\bar{\mathbf{A}}^{(r)} \bar{\phi}^{(r,s)})}. \quad (21)$$

Note that s denotes the iteration number over (21) and we used the diagonal loading technique, i.e., $\bar{\mathbf{A}}^{(r)} = \lambda_m \mathbf{I} - \mathbf{A}^{(r)}$, where the loading parameter $\lambda_m \geq \lambda_{max}(\mathbf{A}^{(r)})$ [31].

Update of ϕ_0 : The Lagrangian function $\mathcal{L}(\phi^{(r)}, \phi_0, \phi_1^{(r-1)}, \mathbf{U}^{(r-1)})$ is quadratic w.r.t ϕ_0 . To show this, from (11) we write $\phi^{(r)H} \bar{\mathbf{Q}}(\Phi_0) \phi^{(r)} = \phi_0^H \bar{\mathbf{Q}}(\Phi^{(r)}) \phi_0$, where

$$\bar{\mathbf{Q}}(\Phi^{(r)}) = \frac{|\alpha_T|^2}{\sigma_r^2} \left(\mathbf{G}^\top \Phi^{(r)\top} \mathbf{a} \mathbf{a}^\top \otimes \mathbf{G}^\top \right)^H \bar{\mathbf{P}} \left(\mathbf{G}^\top \Phi^{(r)\top} \mathbf{a} \mathbf{a}^\top \otimes \mathbf{G}^\top \right) \quad (22)$$

and $\Phi^{(r)} = \text{vec}_{L,L}^{-1}(\mathbf{D}_L \phi^{(r)})$. For the sake of brevity, we denoted $\mathbf{a}(\theta_{h_t}, \theta_{v_t})$ by \mathbf{a} . By substituting (22) in (18), the minimization of the Lagrangian w.r.t ϕ_0 is equivalent to

$$\text{minimize}_{\phi_0 \in \Omega^{L(L+1)/2}} \phi_0^H \bar{\mathbf{R}}^{(r)} \phi_0 + \text{Re}(\bar{\mathbf{c}}^{(r)H} \phi_0), \quad (23)$$

where $\bar{\mathbf{R}}^{(r)} = -\beta \bar{\mathbf{Q}}(\phi^{(r)})$ and $\bar{\mathbf{c}}^{(r)} = -\rho_0 \phi^{(r)}$. Similar to the update for ϕ , by letting $\hat{\mathbf{A}}^{(r)} = \begin{bmatrix} \bar{\mathbf{R}}^{(r)} & \bar{\mathbf{c}}^{(r)}/2 \\ \bar{\mathbf{c}}^{(r)H}/2 & 0 \end{bmatrix}$ and $\bar{\phi}_0 = [\phi_0^\top \ 1]^\top$, similar power method like iterations as in (21), will be applicable to the problem. We have

$$\bar{\phi}_0^{(r,t+1)} = e^{j \arg(\hat{\mathbf{A}}^{(r)} \bar{\phi}_0^{(r,t)})}. \quad (24)$$

where t is the number for power method like iterations and $\hat{\mathbf{A}}^{(r)} = \lambda_m \mathbf{I} - \hat{\mathbf{A}}^{(r)}$, with the loading parameter is chosen such that $\lambda_m \geq \lambda_{max}(\hat{\mathbf{A}}^{(r)})$.

Update of ϕ_1 : Given $\phi^{(r)}, \phi_0^{(r)}, \mathbf{U}^{(r-1)}$, we minimize $\mathcal{L}(\phi^{(r)}, \phi_0^{(r)}, \phi_1, \mathbf{U}^{(r-1)})$ under the finite alphabet constraint $\phi_1 \in \Omega_M^{L^2 \times 1}$. Analogously, we solve

$$\underset{\phi_1 \in \Omega_M^{L(L+1)/2}}{\text{maximize}} \quad \text{Re}(\hat{\mathbf{c}}^{(r)H} \phi_1), \quad (25)$$

where $\hat{\mathbf{c}}^{(r)} = \rho_1 \phi^{(r)}$. Rewrite this problem as

$$\begin{aligned} & \underset{\gamma_l}{\text{maximize}} \quad \cos(\gamma_l - \psi_l) \\ & \text{subject to} \quad \gamma_l \in \left\{ 1, \frac{2\pi}{M}, \dots, \frac{2\pi(M-1)}{M} \right\}, \end{aligned} \quad (26)$$

where γ_l is the phase of $\phi_{1,l}$ and ψ_l is the phase of $\hat{\mathbf{c}}_l^{(r)}$. The solution is obtained by an exhaustive search for m such that $m_l^{(r)} = \underset{m}{\text{argmax}} \cos(2\pi \frac{m}{M} - \psi_l)$, $m \in \{0, \dots, M-1\}$. Then, for $l \in \{1, \dots, L^2\}$, the update of the l -th element in $\phi_1^{(r)}$ is

$$\phi_{1_l}^{(r)} = e^{j2\pi \frac{m_l^{(r)}}{M}}. \quad (27)$$

Update of \mathbf{U} : Consider the following problem

$$\begin{aligned} \mathcal{P}_2 : & \underset{\mathbf{U}}{\text{minimize}} \quad \|\Phi^{(r)} - \mathbf{U}\|_2 \\ & \text{subject to} \quad \mathbf{U}^H \mathbf{U} = \mathbf{I}. \end{aligned} \quad (28)$$

Consider the singular value decomposition (SVD) of $\Phi^{(r)}$ as $\Phi^{(r)} = \mathbf{U}_1 \Sigma \mathbf{U}_2^H$, then the solution of \mathcal{P}_2 is given by [32]

$$\mathbf{U}^{(r)} = \mathbf{U}_2 \mathbf{U}_1^H. \quad (29)$$

Algorithm 1 summarizes the overall design procedure of BD-RIS scattering matrix.

Algorithm 1. Optimal design of BD-RIS scattering matrix for ISAC.

Input Initializations $\phi^{(0)}, \phi_0^{(0)}, \phi_1^{(0)}, \mathbf{U}^{(0)}, r = 1$.

- 1: Set $s = 1$, **while** $\|\bar{\phi}^{(r,s)} - \bar{\phi}^{(r,s+1)}\| > \epsilon$ **do** update $\bar{\phi}^{(r,s)}$ according to (21) and $s = s + 1$.
- 2: $\phi^{(r)} = [\mathbf{I}_{L(L+1)/2} \quad \mathbf{0}] \bar{\phi}^{(r,s)}$.
- 3: Set $t = 1$, **while** $\|\bar{\phi}_0^{(r,t)} - \bar{\phi}_0^{(r,t+1)}\| > \epsilon_1$ **do** update $\bar{\phi}_0^{(r,t)}$ according to (24) and $t = t + 1$.
- 4: Update $\phi_1^{(r)}$ and $\mathbf{U}^{(r)}$ as in (27) and (29), respectively.
- 5: $r = r + 1$.
- 6: Repeat steps 1-5 until a prescribed stop criterion is satisfied, e.g., $\|\phi^{(r)} - \phi^{(r+1)}\| \leq \epsilon_2$.

Output $\Phi^* = \text{vec}_{L,L}^{-1}(\mathbf{D}_L \phi^{(r)})$.

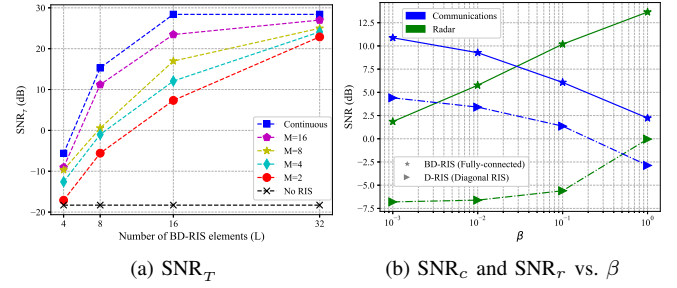


Fig. 2. (a) SNR_T is plotted against the increasing number of elements in BD-RIS. (b) Performance of D-RIS and BD-RIS in terms of SNR_c and SNR_T vs. different values of β .

Remark 1. For continuous-valued scattering matrices i.e. $\phi \in \Omega^{L^2}$, it is sufficient to remove the latent variable ϕ_1 from \mathcal{P}_2 and solve it with respect to ϕ , ϕ_0 and \mathbf{U} .

Remark 2. Contrary to BD-RIS above, D-RIS design [16] is less complex because it introduces a single latent variable to simplify quartic optimization into a quadratic alternative.

V. NUMERICAL EXPERIMENTS

To evaluate our proposed algorithm, we assume the DFBS located at $(0, 0, 0)$ m, in the 3-D Cartesian plane, is equipped with $N = 8$ Tx and Rx antennas with half-wavelength antenna spacing. The ISAC system is serving $K = 4$ single-antenna users located at $(20, 20, 0)$ m and simultaneously detects a Swerling 0 point-like target with complex reflectivity coefficient $\alpha_T \sim \mathcal{CN}(0, 1)$ and located at $(20, 20, 0)$ m. The ISAC system is being assisted by a BD-RIS located at $(30, 30, 0)$ m. The variance of noise at communication users and sensing Rx is set at $\sigma_c^2 = \sigma_r^2 = -100$ dBm. We assumed an i.i.d Rayleigh fading channel in the DFBS to BD-RIS, BD-RIS to users and DFBS to users paths which we abbreviate by RD, UR and UD, respectively. The path loss is modelled as $p_{ij} = p_0 d^{-\alpha_{ij}}$, where p_0 is the path loss at distance 1m and $ij \in \{\text{RD}, \text{UR}, \text{UD}\}$. We set $p_0 = -30$ dB, $\alpha_{\text{RD}} = 2$, $\alpha_{\text{UD}} = 4$ and $\alpha_{\text{UR}} = 2.8$ for the paths that signal propagates through. The CSI matrices are generated according to $\mathbf{G} \sim \mathcal{CN}(0, p_{\text{RD}} \mathbf{I})$, $\mathbf{H} \sim \mathcal{CN}(0, p_{\text{UR}} \mathbf{I})$ and $\mathbf{F} \sim \mathcal{CN}(0, p_{\text{UD}} \mathbf{I})$.

Fig. 2a illustrates the performance of Algorithm 1 for different resolutions of BD-RIS with discrete valued optimized phases in comparison with the continuous phase and no RIS. We set $\beta = 0.5$, and manually tuned the penalty parameters $\rho_i, i \in \{0, \dots, 3\}$ until convergence. To design BD-RIS with continuous phases, we adapt Algorithm 1 as per Remark 1. Fig. 2b shows that fully-connected BD-RIS outperforms conventional D-RIS in terms of the optimized SNR_T and SNR_c . Here, D-RIS is employed with phases optimized according to Remark 2. Moreover, changing β in the interval $[10^{-3}, 1]$ tunes our design criterion. Increasing β shifts the system from communications-centric to radar-centric as evidenced from increasing (decreasing) SNR_T (SNR_c).

REFERENCES

- [1] J. A. Hodge, K. V. Mishra, B. M. Sadler, and A. I. Zaghoul, "Index-modulated metasurface transceiver design using reconfigurable intelli-

- gent surfaces for 6G wireless networks,” *IEEE Journal of Selected Topics in Signal Processing*, vol. 17, no. 6, pp. 1248–1263, 2023.
- [2] J. A. Hodge, K. V. Mishra, and A. I. Zaghoul, “Intelligent time-varying metasurface transceiver for index modulation in 6G wireless networks,” *IEEE Antennas and Wireless Propagation Letters*, vol. 19, no. 11, pp. 1891–1895, 2020.
- [3] S. P. Chepuri, N. Shlezinger, F. Liu, G. C. Alexandropoulos, S. Buzzi, and Y. C. Eldar, “Integrated sensing and communications with reconfigurable intelligent surfaces: From signal modeling to processing,” *IEEE Signal Processing Magazine*, vol. 40, no. 6, pp. 41–62, 2023.
- [4] C. Huang, A. Zappone, G. C. Alexandropoulos, M. Debbah, and C. Yuen, “Reconfigurable intelligent surfaces for energy efficiency in wireless communication,” *IEEE Transactions on Wireless Communications*, vol. 18, no. 8, pp. 4157–4170, 2019.
- [5] W. Shi, J. Xu, W. Xu, C. Yuen, A. L. Swindlehurst, and C. Zhao, “On secrecy performance of RIS-assisted MISO systems over rician channels with spatially random eavesdroppers,” *IEEE Transactions on Wireless Communications*, 2024, in press.
- [6] K. V. Mishra, A. Chattopadhyay, S. S. Acharjee, and A. P. Petropulu, “OptM3Sec: Optimizing multicast IRS-aided multi-antenna DFRC secrecy channel with multiple eavesdroppers,” in *IEEE International Conference on Acoustics, Speech and Signal Processing*, 2022, pp. 9037–9041.
- [7] Z. Esmailbeig, K. V. Mishra, and M. Soltanalian, “IRS-aided radar: Enhanced target parameter estimation via intelligent reflecting surfaces,” in *IEEE Sensor Array and Multichannel Signal Processing Workshop*, 2022, pp. 286–290.
- [8] E. Shtaiwi, H. Zhang, A. Abdelhadi, A. L. Swindlehurst, Z. Han, and H. V. Poor, “Sum-rate maximization for RIS-assisted integrated sensing and communication systems with manifold optimization,” *IEEE Transactions on Communications*, vol. 71, no. 8, pp. 4909–4923, 2023.
- [9] R. Liu, M. Li, Y. Liu, Q. Wu, and Q. Liu, “Joint transmit waveform and passive beamforming design for RIS-aided DFRC systems,” *IEEE Journal of Selected Topics in Signal Processing*, vol. 16, no. 5, pp. 995–1010, 2022.
- [10] K. V. Mishra, M. R. B. Shankar, V. Koivunen, B. Ottersten, and S. A. Vorobyov, “Toward millimeter-wave joint radar communications: A signal processing perspective,” *IEEE Signal Process. Mag.*, vol. 36, no. 5, pp. 100–114, 2019.
- [11] A. Liu, Z. Huang, M. Li, Y. Wan, W. Li, T. X. Han, C. Liu, R. Du, D. K. P. Tan, J. Lu, Y. Shen, F. Colone, and K. Chetty, “A survey on fundamental limits of integrated sensing and communication,” *IEEE Communications Surveys & Tutorials*, vol. 24, no. 2, pp. 994–1034, 2022.
- [12] F. Liu, Y. Cui, C. Masouros, J. Xu, T. X. Han, Y. C. Eldar, and S. Buzzi, “Integrated sensing and communications: Toward dual-functional wireless networks for 6G and beyond,” *IEEE Journal on Selected Areas in Communications*, vol. 40, no. 6, pp. 1728–1767, 2022.
- [13] X. Hu, C. Liu, M. Peng, and C. Zhong, *Reconfigurable intelligent surface-enabled integrated sensing and communication in 6G*. Springer, 2024.
- [14] R. Liu, M. Li, Q. Liu, and A. L. Swindlehurst, “SNR/CRB-constrained joint beamforming and reflection designs for RIS-ISAC systems,” *arXiv preprint arXiv:2301.11134*, 2023.
- [15] T. Wei, L. Wu, K. V. Mishra, and M. B. Shankar, “Multi-IRS-aided Doppler-tolerant wideband DFRC system,” *IEEE Transactions on Communications*, vol. 71, no. 11, pp. 6561–6577, 2023.
- [16] Z. Esmailbeig, A. Eamaz, K. V. Mishra, and M. Soltanalian, “Quantized phase-shift design of active IRS for integrated sensing and communications,” in *IEEE International Conference on Acoustics, Speech, and Signal Processing Workshops*, 2023, pp. 1–5.
- [17] M. Hua, Q. Wu, C. He, S. Ma, and W. Chen, “Joint active and passive beamforming design for IRS-aided radar-communication,” *IEEE Transactions on Wireless Communications*, vol. 22, no. 4, pp. 2278–2294, 2022.
- [18] S. Shen, B. Clerckx, and R. Murch, “Modeling and architecture design of reconfigurable intelligent surfaces using scattering parameter network analysis,” *IEEE Transactions on Wireless Communications*, vol. 21, no. 2, pp. 1229–1243, 2022.
- [19] M. Nerini, S. Shen, and B. Clerckx, “Closed-form global optimization of beyond diagonal reconfigurable intelligent surfaces,” *IEEE Transactions on Wireless Communications*, vol. 23, no. 2, pp. 1037–1051, 2024.
- [20] H. Li, S. Shen, and B. Clerckx, “Beyond diagonal reconfigurable intelligent surfaces: From transmitting and reflecting modes to single-, group-, and fully-connected architectures,” *IEEE Transactions on Wireless Communications*, vol. 22, no. 4, pp. 2311–2324, 2023.
- [21] Q. Wu, T. Q. Duong, D. W. K. Ng, R. Schober, and R. Zhang, *Intelligent surfaces empowered 6G wireless network*. John Wiley & Sons, 2023.
- [22] T. Fang and Y. Mao, “A low-complexity beamforming design for beyond-diagonal RIS aided multi-user networks,” *IEEE Communications Letters*, vol. 28, no. 1, pp. 203–207, 2024.
- [23] B. Wang, H. Li, S. Shen, Z. Cheng, and B. Clerckx, “A dual-function radar-communication system empowered by beyond diagonal reconfigurable intelligent surface,” *arXiv preprint arXiv:2301.03286*, 2023.
- [24] I. Santamaria, M. Soleymani, E. Jorswieck, and J. Gutiérrez, “SNR maximization in beyond diagonal RIS-assisted single and multiple antenna links,” *IEEE Signal Processing Letters*, vol. 30, pp. 923–926, 2023.
- [25] J. A. Zhang, F. Liu, C. Masouros, R. W. Heath, Z. Feng, L. Zheng, and A. Petropulu, “An overview of signal processing techniques for joint communication and radar sensing,” *IEEE Journal of Selected Topics in Signal Processing*, vol. 15, no. 6, pp. 1295–1315, 2021.
- [26] J. Liu, K. V. Mishra, and M. Saquib, “Co-designing statistical MIMO radar and in-band full-duplex multi-user MIMO communications,” *arXiv preprint arXiv:2006.14774*, 2020.
- [27] A. R. Chiriyath, B. Paul, and D. W. Bliss, “Radar-communications convergence: Coexistence, cooperation, and co-design,” *IEEE Transactions on Cognitive Communications and Networking*, vol. 3, no. 1, pp. 1–12, 2017.
- [28] M. Nerini, S. Shen, and B. Clerckx, “Discrete-value group and fully connected architectures for beyond diagonal reconfigurable intelligent surfaces,” *IEEE Transactions on Vehicular Technology*, vol. 72, no. 12, pp. 16 354–16 368, 2023.
- [29] M. I. Skolnik, *Radar handbook*, 3rd ed. McGraw-Hill, 2008.
- [30] X. Yu, G. Cui, J. Yang, J. Li, and L. Kong, “Quadratic optimization for unimodular sequence design via an ADPM framework,” *IEEE Transactions on Signal Processing*, vol. 68, pp. 3619–3634, 2020.
- [31] M. Soltanalian and P. Stoica, “Designing unimodular codes via quadratic optimization,” *IEEE Transactions on Signal Processing*, vol. 62, no. 5, pp. 1221–1234, 2014.
- [32] H. He, P. Stoica, and J. Li, “Designing unimodular sequence sets with good correlations – Including an application to MIMO radar,” *IEEE Transactions on Signal Processing*, vol. 57, no. 11, pp. 4391–4405, 2009.